

## **Observation of the soft mode behavior across the structural phase transition in the excitonic insulator Ta<sub>2</sub>NiSe<sub>5</sub>**

Min-Jae Kim<sup>1,2</sup>, Armin Schulz<sup>1</sup>, Tomohiro Takayama<sup>1,3</sup>, Masahiko Isobe<sup>1</sup>, Hidenori Takagi<sup>1,3,4</sup>, and Stefan Kaiser<sup>1,2</sup>

<sup>1</sup> Max Planck Institute for Solid State Research, Stuttgart, Germany

<sup>2</sup> 4<sup>th</sup> Physics Institute, University of Stuttgart, Germany

<sup>3</sup> Institute for Functional Matter and Quantum Technologies, University of Stuttgart, Germany

<sup>4</sup> Department of Physics, University of Tokyo

Ta<sub>2</sub>NiSe<sub>5</sub> became one of the most investigated candidate materials for hosting an excitonic insulator ground state. Many studies describe the corresponding phase transition as a condensation of excitons breaking a continuous symmetry. This view got challenged recently pointing out the importance of the loss of two mirror symmetries at a structural phase transition that occurs together with the semiconductor – excitonic insulator transition. For such a scenario an unstable optical zone-center phonon at low energy is proposed to drive the transition. Here we report on the experimental observation of such a soft mode behavior using Raman spectroscopy. In addition we find a novel spectral feature, likely of electronic or joint electronic and phononic origin, that is clearly distinct from the lattice dynamics and that becomes dominant at T<sub>c</sub>.

*Introduction* - Recently the possibility of realizing the elusive state of an excitonic insulator (EI) in the zero-gap semiconductor Ta<sub>2</sub>NiSe<sub>5</sub> (TNSe) has stimulated a tremendous body of experimental and theoretical work. An EI consists of condensed excitons forming a new phase of matter whose proposed macroscopic quantum states may resemble many properties of superconductors and superfluids [1-7]. Besides this interesting test bed for many-body physics, the ultrafast response in TNSe under laser-excitation is a potential platform for novel optoelectronic applications [8,9]. An EI transition by spontaneous condensation of excitations is expected in narrow bandwidth semimetals or small bandgap semiconductors if the exciton binding energy exceeds the bandwidth or the bandgap of the system. EIs have been realized in specifically designed electron-hole bilayer systems [10-14] or by creating high exciton densities under strong photoexcitation [15-17]. However, identifying fingerprint of EI phases in bulk materials remain an experimental challenge. Prominent candidate materials like 1T-TiSe<sub>2</sub> show an indirect band gap and therefore the potential EI state appears together with a charge density wave (CDW) that seems to drive the dynamics [18,19]. In contrast, Ta<sub>2</sub>NiSe<sub>5</sub> (TNSe) is a direct band gap semiconductor that has been proposed to show an EI transition without charge, or other finite momentum order [20,21]. A semiconductor-insulator transition appears at  $T_c = 328\text{K}$  that can be tuned via chemical or physical pressure [22, 23]. Evidence for excitonic condensation comes from a characteristic band flattening seen in angle resolved photoemission [24-26] and the opening of a gap in electronic [8,27] and optical [28-31] spectra. Further fingerprints stem from characteristic non-equilibrium responses of the ground state that are compatible with the melting and relaxation dynamics of a condensate [32-35] and the excitation of possible collective modes of a coherent ground state [31,36,37]. Nevertheless, the origin of the gap is still under debate due to a structural phase transition from a high-temperature orthorhombic to a low-temperature monoclinic phase that happens simultaneously at  $T_c$  despite the absence of CDW [8,21,38]. TNSe crystallizes as a quasi-one-dimensional structure of Ta-Ni-Ta chains. In the low-temperature phase two mirror symmetries of the high-temperature phase are broken by a shear motion of the Ta against the Ni chains [see insets of Figure 1]. Using inelastic x-ray measurements Nakano et al. [38] show that this displacement can be decomposed into B<sub>2g</sub> phonons of the high-temperature phase. While

they find a significant frequency jump of the transverse acoustic mode describing the Se atom motion when approaching the phase transition from the high temperature side they cannot evidence a softening in the optical phonon mode in the temperature range they accessed. The latter mode describes the Ta atom shear motion that happens at the phase transition. But a strong linewidth broadening of this mode indicates strong electron phonon coupling. A strong lattice interaction is also evidenced by strong Fano resonances [29] and polaronic bands [30] in optics or the lattice coupled dynamics of the non-equilibrium responses [31,32,36, 37]. The proposed scenario for the EI in TNSe is that the excitonic condensate couples to the lattice phonons and as such drives a joint excitonic and structural instability [23,28,39]. However, this picture of exciton condensation driven by pure electronic Coulomb interactions of the electron hole pairs got recently challenged. Exciton condensation would require breaking a continuous symmetry and a complex order parameter to describe the low-temperature phase of TNSe. In particular Mazza et al. [40] and Watson et al. [41] point out the loss of two mirror symmetries in the low temperature phase are linked to a discrete symmetry break. They propose possible excitonic (linearly coupled to lattice modes) and structural instabilities that are in agreement with the experimental observations of Nakano et al. [38]. Both instabilities lead to a hybridization of the Ta and Ni bands in the center of the Brillouin zone in contrast to the pure bands in a condensation scenario. A theoretical density functional theory study by Subedi [42] has recently explored the corresponding zone center optical phonon branches relevant for this case and suggests that the optical B2g modes could drive the phase transition. According to the calculations, if the B2g phonon mode softens as the Tc is approached from above, the dynamical instability is due to an unstable optical phonon mode. No softening should be observed if the instability is electronic or due to an unstable elastic mode corresponding to a uniform shear distortion of the lattice. However clear experimental fingerprints for the dynamics of such instabilities are missing.

This motivates our Raman scattering studies on TNSe presented here to explore the crucial soft mode behavior in an energy range down to 20 cm<sup>-1</sup>. We clearly identify the presence of a B2g soft mode above Tc and we report on and characterize an additional broad either electronic or unusual broadened coupled electronic-phononic feature that

appears next to the soft mode but that exists across the phase transition.

*Experiment* - Single crystals of Ta<sub>2</sub>NiSe<sub>5</sub> were grown by chemical vapor transport reaction described in [22]. The linear Raman spectrum was measured using a Jobin Yvon Typ V 010 LabRAM single grating spectrometer, equipped with a double super razor edge filter and a Peltier-cooled charge-coupled device camera. The resolution of the spectrometer (grating, 1800 lines/mm) was 1cm<sup>-1</sup>. The spectra were taken in a quasi-backscattering geometry using the linearly polarized 632.817-nm line of a He/Ne gas laser. The power was lower than 1 mW, and the spot size was 10 mm. The scattered signal was filtered and analyzed using an additional polarizer before the spectrometer. The experimental configurations Y(XX)Y and Y(XZ)Y probe only Ag representations in the monoclinic phase (C2/c) and Ag, B2g channel respectively in the orthorhombic phase (cmcm) of TNSe. The Z(YX)Z configuration accesses the Bg channel in the monoclinic phase and B1g channel in the orthorhombic phase.

*Results* - Figure 1 shows the Raman spectra of TNSe in Y(X-) geometry in the temperature range from 10 to 800 K. In the high temperature regime that goes clearly beyond the existing temperature range of 400 K covered in the inelastic x-ray measurements of Ref. [38]. The blue spectra are taken in the monoclinic phase (sketched as inset) below T<sub>c</sub> and belong in the given experimental geometry to the Ag channel. Above T<sub>c</sub> spectra are shown in red and are taken in the orthorhombic phase (sketched as inset) so that in this geometry the experiment probes the Ag and B2g channel. Starting below T<sub>c</sub> shows clear peaks at 101, 124, 136, 149, 180, 195cm<sup>-1</sup> identified as Ag symmetries already in earlier studies [8, 43] On increasing temperature the high frequency modes do not show strong changes up to T<sub>c</sub> except the modes at 124 and 136cm<sup>-1</sup> which shift to lower energy and broaden. At the same time they decrease in amplitude. Above T<sub>c</sub> the 124 cm<sup>-1</sup> mode disappears while the 136 cm<sup>-1</sup> mode shows up to the highest temperature. Increasing the temperature further shows a slight redshift and broadening of the mode. The 101 cm<sup>-1</sup> mode above T<sub>c</sub> shows a similar trend. This behavior is in agreement and already known from the previous studies [43]. Here we will focus in particular on the so far unexplored low frequency response with prominent peaks at 36cm<sup>-1</sup> and 71cm<sup>-1</sup> below T<sub>c</sub>. The 36 cm<sup>-1</sup> Ag mode is known as a peculiar mode that

under strong impulsive excitation shows a coupling to the excitonic system and resembles amplitude mode like behavior [31]. However, in agreement with reports in the non-equilibrium study, in the equilibrium measurements this mode shows basically no change of width nor a shift in frequency as function of temperature. In amplitude the equilibrium mode increases as function of increasing temperature in stark contrast to the non-linear excitation.

*Ag and B2g low frequency spectra.* However the 71 cm<sup>-1</sup> mode and the spectral range right below will become the dominant key features of the transition. Below T<sub>c</sub>, in the monoclinic phase, shown as the blue spectra in Fig. 1 barely any change is visible in the mode on increasing temperature except for a small redshift on approaching T<sub>c</sub>. Hardly noticeable but already present below T<sub>c</sub> is a small broad background of spectral weight in the frequency range from 42-71 cm<sup>-1</sup>. The weight of this unknown feature increases towards T<sub>c</sub>. Above T<sub>c</sub> in the orthorhombic phase, shown in the red spectra, very prominent changes happen. Across the phase transition the mode at 71cm<sup>-1</sup> is strongly suppressed and the unknown broad spectral feature becomes clearly visible next to this mode. On further temperature increase in the orthorhombic phase, the broad spectral feature is most prominent between 330 and 400 K before an additional peak appears on top of the broad background and becomes sharper and dominant on increasing temperature.

To understand and fully characterize this new and anomalous broad features as well as the appearing new modes we are going to map each symmetry channel individually. Figure 2 shows the polarization-dependent Raman spectra in the monoclinic phase below T<sub>c</sub> at 300 K and in the orthorhombic phase above T<sub>c</sub> at 400 K. In the XX configuration at 300K the well-known sharp Ag modes at 36, 101, 124cm<sup>-1</sup> and the other high frequency modes are visible. The YX configuration of the Bg channel besides the Bg modes shows some leakage of peaks from the XX configuration because of the quasi quasi-one-dimensional crystal structure of the real system. But these are not in the focus of the present manuscript. Most important the XZ configuration does not show strong leakage of modes of other configurations. In this channel the 71 cm<sup>-1</sup> Ag mode as well as the broad background feature are clearly visible. As mentioned before the feature is present

already for temperatures below  $T_c$ . Above  $T_c$  at 400K Ag and B1g channels in XX and YX geometries show the already known high frequency phonons. Notable is again the XZ channel that probes the B2g channel above  $T_c$ . In the low frequency range the sharp peak at 71cm<sup>-1</sup> disappears and the remarkable broad background feature arises above  $T_c$ .

Since both key features, the 71 cm<sup>-1</sup> Ag mode and the broad new feature all appear only in the XZ channel we plot the temperature dependent spectra of this channel across the whole studies temperature range in Fig. 3. Below  $T_c$  (green/yellow spectra), probing the Ag channel we find the sharp phonon modes at 71 cm<sup>-1</sup> and the high frequency modes at 101, 124, 136, 149, 180, 195 cm<sup>-1</sup>. On increasing temperature the Ag modes in the XZ configuration become suppressed and disappears at  $T_c$ . This is in full agreement since XZ probes the B2g channel above  $T_c$ . The Ag modes remain in the XX configuration at 400K that probes the Ag channel above  $T_c$  (black spectrum). In the B2g channel of the XZ geometry above  $T_c$  (orange/red spectra) new small modes appear at 96 and 150cm<sup>-1</sup> that are distinct from possible leakage but of unknown origin. Most prominent is the appearance of the broad background feature at temperatures up to 400 K and the additional new peak around 60 cm<sup>-1</sup> on further temperature increase.

*Characterization of the modes* – In the following we are going to present the fit of the temperature dependence of the Raman spectra. All phonon modes are fit using single Gaussian functions. However the anomalous broad spectral feature is difficult to capture. It can be fit either using multiple Gaussians (where the number of fit parameters becomes large) or as we have done here using a super Gaussian function. Figure 4 shows the significant low frequency Raman spectra in the XZ geometry and the extracted fit parameters for three features: (1) As key feature at highest temperatures we clearly identify a strong sharp B2g phonon mode at 60cm<sup>-1</sup> (blue). On decreasing temperature this mode clearly softens to 52 cm<sup>-1</sup> and significantly broadens approaching  $T_c$ . Its intensity decreases and disappears at  $T_c$ . This soft mode we classify as the B2g zone-center optical phonon mode predicted by Subedi [42]. The inelastic x-ray study [38] did not find this unstable B2g mode in the range of 328-400K since it already softened and broadened significantly. Also within our data we cannot resolve the mode anymore below 400 K. (2) However, at 400 K we see the onset of a new mode that evolves into the 71

cm<sup>-1</sup> (2 THz) Ag mode in the monoclinic phase below T<sub>c</sub> (green) where the mode suddenly sharpens at the phase transition. In line with the interpretation of Subedi this new mode in the monoclinic phase corresponds to the amplitude modulation of the order parameter deriving from the unstable B<sub>2g</sub> mode of the orthorhombic phase [42]. The most surprising feature in TNSe is (3) the anomalous broad spectral component that dominates the weight in the temperature range around the phase transition (red). At very high temperatures it clearly exists with a strong finite weight next to the soft mode. When cooling below 450 K its weight significantly increases and it becomes the dominant feature when approaching T<sub>c</sub>. Then its intensity significantly drops at T<sub>c</sub> but remaining comparable to other modes even below T<sub>c</sub>, as seen e.g. at the 300 K data. Only when cooling further down the relative weight decreases further but still finite down to lowest temperatures. As mentioned this feature is fit using a super-Gaussian contribution so that it is difficult to assign. Possibilities are fluctuations that are small in the low-temperature ordered phase that significantly increase and peak at T<sub>c</sub> and remain very prominent even for temperatures far above T<sub>c</sub>. As the feature also could be fit with multiple peaks it also could represent other yet unidentified phonon modes that in the high temperature phase are suppressed from the strong soft mode behavior. Interesting to note is that laser heating the system with high power in the Raman experiment the broad spectral feature shows a heating response that is more susceptible to the fluence than the pure phononic system. That indicates an electronic or joint electronic-phononic origin and has to be examined in future studies.

To contrast the soft mode instability driving the structural phase transition and the appearance of a new mode in the monoclinic low-temperature phase of TNSe we show the phonon mode behavior in the sister compound Ta<sub>2</sub>NiS<sub>5</sub> (TNS). TNS is a semiconductor that does not show an excitonic nor a structural phase transition [22]. Here only an equivalent 2 THz mode appears. Its behavior (grey) shows a roughly monotonic increase in intensity and only a slight red-shift on cooling across the measured temperature range. Also the mode stays always very sharp in the whole temperature range.

*Conclusion* – We have performed a detailed study of the low frequency lattice dynamics across the orthorhombic to monoclinic structural phase transition in Ta<sub>2</sub>NiSe<sub>5</sub>. We can clearly identify a B<sub>2g</sub> optical zone-center phonon soft mode in the orthorhombic phase at temperatures above T<sub>c</sub>. This observation underlines a proposed mechanism by Subedi [42] that this instability could act as a prime cause for the structural phase transition; leading to the appearance of a new A<sub>g</sub> mode in the monoclinic phase below T<sub>c</sub>, which we also clearly observe. Interestingly this change between the different modes in their specific symmetry channels seems not to happen abruptly at T<sub>c</sub> but smeared out around the structural phase transition. Right in that regime a broad new spectral feature in the low frequency regime dominates that might trace fluctuating electronic or fluctuating joint electronic and structural order.

**Acknowledgements** We thank A. Subedi and A. V. Boris for insightful discussions.

## References

- [1] N. F. Mott, *Philos. Mag.* 6, 287 (1961).
- [2] Keldysh *Sov. Phys. Solid St* 6 2219 (1965).
- [3] D. Jérôme, T. M. Rice, and W. Kohn, *Phys. Rev.* 158, 462 (1967).
- [4] B. I. Halperin and T. M. Rice, *Rev. Mod. Phys.* 40, 755 (1968).
- [5] F. X. Bronold and H. Fehske, *Phys. Rev.* B74, 165107 (2006).
- [6] K. Seki, R. Eder, and Y. Ohta, *Phys. Rev.* B84, 245106 (2011).
- [7] B. Zenker, D. Ihle, F. X. Bronold, and H. Fehske, *Phys. Rev. B* 85, 121102(R) (2012).
- [8] S. Y. Kim, Y. Kim, C.-J. Kang, E.-S. An, H. K. Kim, M. J. Eom, M. Lee, C. Park, T.-H. Kim, H. C. Choi, B. I. Min, and J. S. Kim, *ACS Nano* 10, 8888 (2016).
- [9] L. Li, W. Wang, L. Gan, N. Zhou, X. Zhu, Q. Zhang, H. Li, M. Tian, T. Zhai, *Adv. Funct. Mater* 26 45 (2016).
- [10] S. De Palo, F. Rapisarda, and Gaetano Senatore *Phys. Rev. Lett.* 88, 206401 (2002).
- [11] J. P. Eisenstein and A. H. MacDonald *Nature* volume 432, 691–694 (2004).
- [12] J. J. Su and A. H. MacDonald *Nat. Phys.* 4 799 (2008).
- [13] D. Nandi, A. D. K. Finck, J. P. Eisenstein, L. N. Pfeiffer & K. W. West *Nat.* 488 481–484 (2012).
- [14] A. Perali, D. Neilson, and A. R. Hamilton *Phys. Rev. Lett.* 110, 146803 (2013).
- [15] D. Snoke, *Science* 298, 1368 (2002).
- [16] L. V. Butov, C. W. Lai, A. L. Ivanov, A. C. Gossard, and D. S. Chemla, *Nat.* 417, 47 (2002).
- [17] L.V. Butov, A. C. Gossard, and D. S. Chemla, *Nature (London)* 418, 751 (2002).
- [18] A. Wilson *Solid State Commun.* 22 551 (1977).

- [19] H. Cercellier, C. Monney, F. Clerc, C. Battaglia, L. Despont, M. G. Garnier, H. Beck, P. Aebi, L. Patthey, H. Berger, and L. Forró *Phys. Rev. Lett.* 99, 146403 (2007).
- [20] S.A. Sunshine, J.A. Ibers *Inorg. Chem.*, 24 3611 (1985).
- [21] F. J. Di Salvo, C. H. Chen, and R. M. Fleming, *J. Less-Common Met.* 116, 51 (1986).
- [22] Y. F. Lu, H. Kono, T. I. Larkin, A. W. Rost, T. Takayama, A. V. Boris, B. Keimer and H. Takagi, *Nat. Comm.* 8 14408 (2017).
- [23] K. Sugimoto, N. Maejima, A. Machida, T. Watanuki, and H. Sawa, *IUCrJ* 5, 158 (2018).
- [24] K. Seki, Y. Wakisaka, T. Kaneko, T. Toriyama, T. Konishi, T. Sudayama, N. L. Saini, M. Arita, H. Namatame, M. Taniguchi, N. Katayama, M. Nohara, H. Takagi, T. Mizokawa, and Y. Ohta, *Phys. Rev. B* 90, 155116 (2014).
- [25] Y. Wakisaka, T. Sudayama, K. Takubo, T. Mizokawa, M. Arita, H. Namatame, M. Taniguchi, N. Katayama, M. Nohara, and H. Takagi, *Phys. Rev. Lett.* 103, 026402 (2009).
- [26] K. Fukutami, R. Stania, J. Jung, E. F. Schwier, K. Shimada, C. I. Kwon, J. S. Kim, H. W. Yeom *Phys. Rev. Lett* 123 206401 (2019).
- [27] J. Lee, C.-J. Kang, M. J. Eom, J. S. Kim, B. I. Min, and H. W. Yeom, *Phys. Rev. B* 99, 075408 (2019).
- [28] K. Sugimoto, S. Nishimoto, T. Kaneko, and Y. Ohta, *Phys. Rev. Lett.* 120, 247602 (2018).
- [29] T. I. Larkin, A. N. Yaresko, D. Pröpper, K. A. Kikoin, Y. F. Lu, T. Takayama, Y. L. Mathis, A. W. Rost, H. Takagi, B. Keimer, and A. V. Boris, *Phys. Rev. B* 95, 195144 (2017).
- [30] T. I. Larkin, R. D. Dawson, M. Höppner, T. Takayama, M. Isobe, Y. L. Mathis, H. Takagi, B. Keimer, and A. V. Boris, *Phys. Rev. B* 98, 125113 (2018).
- [31] D. Werdehausen, T. Takayama, M. Höppner, G. Albrecht, A. W. Rost, Y. Lu, D. Manske, H. Takagi, and S. Kaiser, *Sci. Adv.* 4, eaap8652 (2018).
- [32] D. Werdehausen, T. Takayama, G. Albrecht, Y. Lu, H. Takagi, and S. Kaiser, *J. Phys.: Condens. Matter* 30, 305602 (2018).
- [33] S. Mor, M. Herzog, D. Golež, P. Werner, M. Eckstein, N. Katayama, M. Nohara, H. Takagi, T. Mizokawa, C. Monney, and J. Stähler, *Phys. Rev. Lett.* 119, 086401 (2017).
- [34] K. Okazaki, Y. Ogawa, T. Suzuki, T. Yamamoto, T. Someya, S. Michimae, M. Watanabe, Y.-F. Lu, M. Nohara, H. Takagi, N. Katayama, H. Sawa, M. Fujisawa, T. Kanai, N. Ishii, J. Itatani, T. Mizokawa, and S. Shin, *Nat. Commun.* 9, 4322, (2018).
- [35] S. Mor, M. Herzog, J. Noack, N. Katayama, M. Nohara, H. Takagi, A. Trunschke, T. Mizokawa, C. Monney, and J. Stähler, *Phys. Rev. B* 97, 115154 (2018).
- [36] D. Werdehausen, S. Y. Agustsson, M. –J. Kim, P. Shabestari, E. Huang, A. Pokharel, T. Larkin, A. Boris, T. Takayama, Y. Lu, A.s W. Rost, H. Chu, A. Yaresko, M. Höppner, A. Schulz, D. Manske, B. Keimer, H. Takagi, S. Kaiser *Proc. SPIE* 10638, Ultrafast Bandgap Photonics III; 1063803 (2018)

- [37] P. Andrich, H. M. Bretscher, Y. Murakami, D. Golež, B. Remez, P. Telang, A. Singh, L. Harnagea, N. R. Cooper, A. J. Millis, P. Werner, A. K. Sood, A. Rao preprint (2020) at <https://arxiv.org/abs/2003.10799>
- [38] A. Nakano, T. Hasegawa, S. Tamura, N. Katayama, S. Tsutsui, and H. Sawa, Phys. Rev. B 98, 045139 (2018).
- [39] T. Kaneko, T. Toriyama, T. Konishi, and Y. Ohta, Phys. Rev. B 87, 035121 (2013).
- [40] G. Mazza, M. Rösner, L. Windgätter, S. Latini, H. Hübener, A. J. Millis, A. Rubio, A. Georges Phys. Rev. Lett. 124, 197601 (2020) .
- [41] M. D. Watson, I. Marković, E. A. Morales, P. Le Fèvre, M. Merz, A. A. Haghighirad, and P. D. C. King, Phys.Rev.Res. 2 13236 (2020).
- [42] A. Subedi preprint at <https://arxiv.org/abs/2002.08352> (2020)
- [43] J. Yan, R. Xiao, X. Luo, H. Lv, R. Zhang, Y. Sun, P. Tong, W. Lu, W. Song, X. Zhu, and Y. Sun, Inorg. Chem 58 9036 (2019).

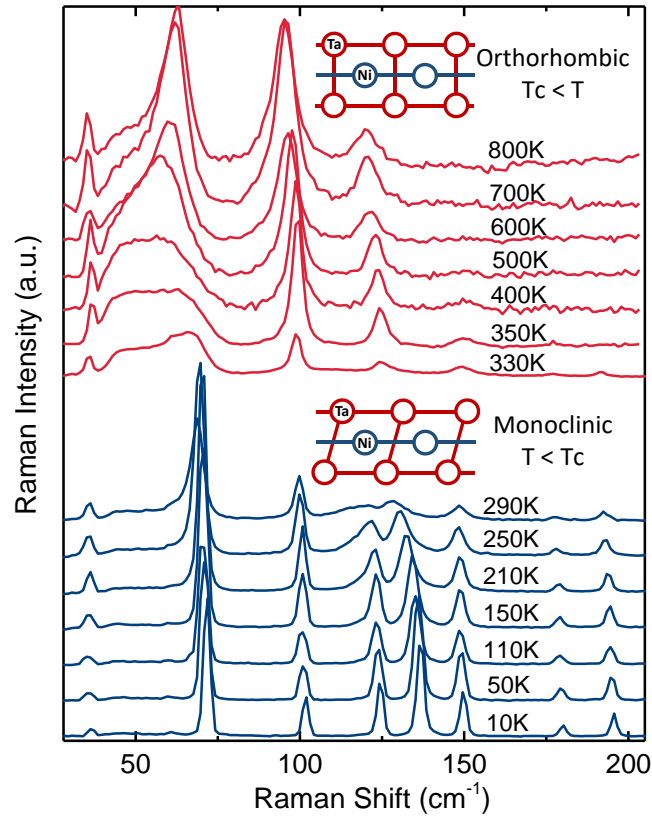


Figure 1. Raman spectrum of Ta<sub>2</sub>NiSe<sub>5</sub> in the orthorhombic phase above (red) and in the monoclinic phase below (blue) the structural phase transition at T<sub>c</sub>=328 K. At the phase transition the Ta chains perform a shear displacement with respect to the Ni chain. The corresponding crystal structures are shown as insets. Spectra are taken in (X-) geometry revealing the A<sub>g</sub> channel below and A<sub>g</sub>+B<sub>2g</sub> channel above T<sub>c</sub>.

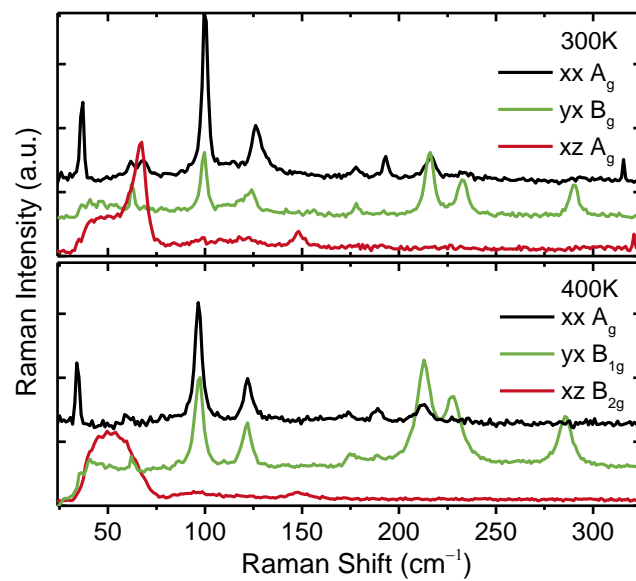


Figure 2. Raman spectra at 300 K in the monoclinic and at 400 K in the orthorhombic phase decomposed into different symmetry channels.

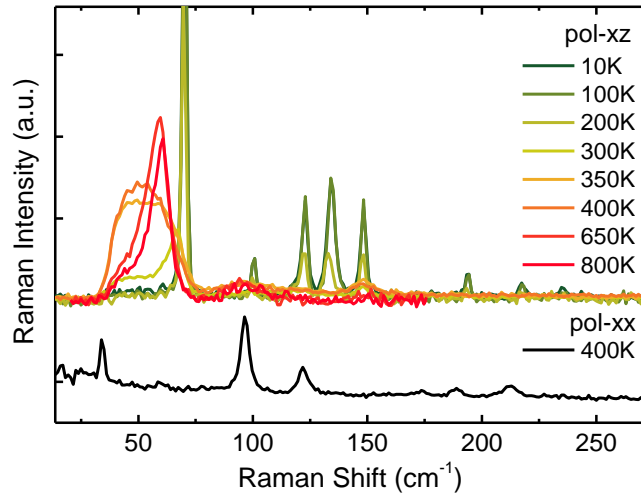


Figure 3. Temperature dependent Raman spectra in the (XZ) geometry probing the Ag channel in the orthorhombic phase below  $T_c$  and the B2g channel above  $T_c$ . The Ag channel above  $T_c$  is shown for 400 K in (XX) geometry.

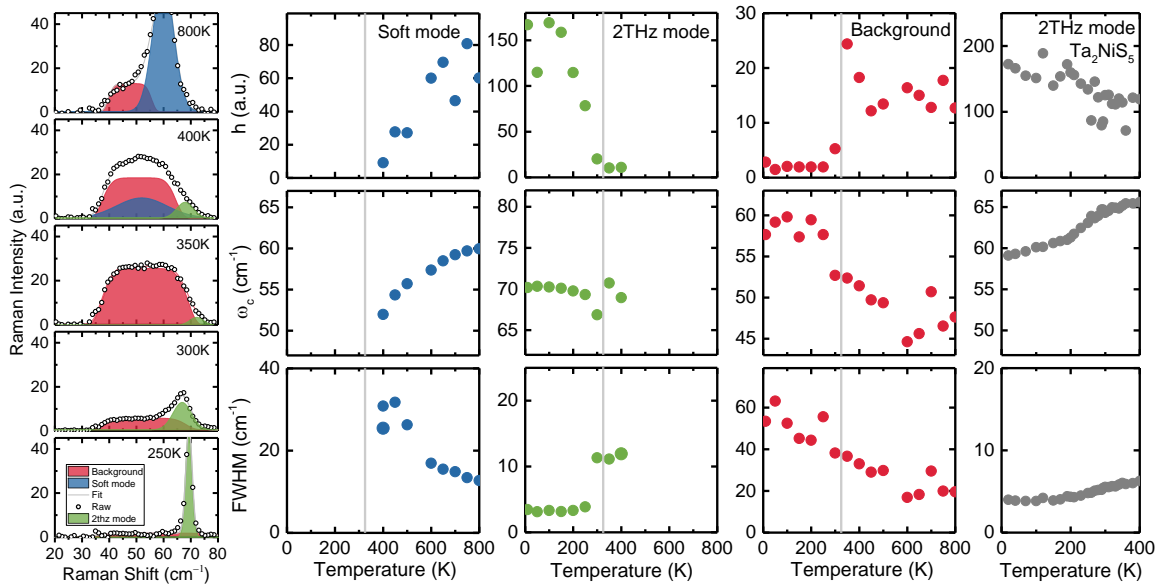


Figure 4. Fit to the low frequency Raman dynamics in the (XZ) channel. Exemplary spectra and extracted parameters of amplitude center frequency and width of the different modes. The key contributions are (1) zone-center B2g soft phonon mode above  $T_c$  (blue), and (2) a 2 THz Ag mode interpreted as amplitude modulation of the order parameter deriving from the unstable B2g mode. In addition (3) a broad spectral feature (red) next to these modes appears across the phase transition with its intensity becoming dominant at  $T_c$ . For comparison the dynamics of the 2THz mode in TNS are given which does not undergo any phase transition.